ARTICLE

Population Change of OH and H_2O in Water Vapor Glow Discharge Measured Using Concentration Modulation Spectroscopy

Bao Li[a], Li Wang[a], Bo Fang[b], Wei-xiong Zhao[b], Lun-hua Deng[a*], Huai-liang Xu[a,c]

a. State Key Laboratory of Precision Spectroscopy, East China Normal University, Shanghai 200062, China
b. Laboratory of Atmospheric Physico-Chemistry, Anhui Institute of Optics and Fine Mechanics, Chinese Academy of Sciences, Hefei 230031, China
c. State Key Laboratory on Integrated Optoelectronics, College of Electronic Science and Engineering, Jilin University, Changchun 130012, China

(Dated: Received on January 15, 2020; Accepted on March 3, 2020)

A distributed feedback laser with a wavelength of 2.8 μm was used to measure the species produced by water vapor glow discharge. Only the absorption spectra of OH radicals and transient H_2O molecules were observed using concentration modulation (CM) spectroscopy. The intensities and orientations of the absorption peaks change with the demodulation phase, but the direction of one absorption peak of H_2O is always opposite to the other peaks. The different spectral orientations of OH and H_2O reflect the increase or the decrease of the number of particles in the energy levels. If more transient species can be detected in the discharge process, the dynamics of excitation, ionization, and decomposition of H_2O can be better studied. This study shows that the demodulation phase relationship of CM spectrum can be used to study the population change of molecular energy levels.

Key words: Glow discharge, OH radical, Concentration modulation spectroscopy, Population change

I. INTRODUCTION

The hydroxyl free radical (OH) exists widely in nature, and it is one of the most important oxidants in the atmosphere. It is not only an important indicator of atmospheric oxidation ability, but also an index of the self-cleaning ability of trace gases [1–3]. The reaction process of OH radical can affect regional and global climate change, atmospheric oxidation level, acid deposition, and other major environmental issues. However, OH radical is difficult to be measured because of its short lifetime (less than 1 s) and low concentration in the atmosphere (in the order of 10^6 molecules/cm^3). Therefore, many researchers invented a variety of methods to generate high concentration OH radical in the laboratory, including photodegradation, discharge, pyrolysis and chemical reaction, so as to simulate the environment in the atmosphere and provide a stable OH source for further study of the dynamic reaction process.

On the earth, water is a primary requisite for living species and the most abundant substance. In spectral experiments, it is also often used to generate transient radicals with high oxidation activity, such as oxygen atoms, ozone molecules, and OH radicals [4–7]. However, there are many kinds of transient molecules generated by discharging poly-atomic parent molecules, even if the same transient molecules will have transitions between different electronic states, resulting in a large number of spectral lines intertwined. Up to now, many methods have successfully distinguished OH radicals from them, such as optical emission spectroscopy (OES) [8], laser-induced fluorescence (LIF) [9–11], electron spin resonance (ESR) [12, 13], and absorption spectroscopy [14–16]. Compared with direct absorption spectroscopy, concentration modulation spectroscopy (CMS) is a form of absorption spectroscopy used to suppress the interference of laser amplitude fluctuation noise and plasma noise during discharge. The CMS is an accompanying technique of the velocity modulation spectroscopy [17, 18].

We produced OH radicals by discharging the flowing water vapor, and observed the spectrum of related species using a mid-infrared (MIR) laser operating at 2.8 μm. The MIR spectrum exactly corresponds to the range of molecular fundamental frequency transitions. In MIR, the line intensities of OH are two orders of magnitude larger than that in the near-infrared (NIR). The molecular absorption of OH in MIR is the strongest, so the MIR spectrum is optimal for qualitative measurement of OH radicals. Due to the limitation of our laser source, only the spectra from OH and H_2O were

*Author to whom correspondence should be addressed. E-mail: lhdeng@phy.ecnu.edu.cn

DOI:10.1063/1674-0068/cjcp2001010

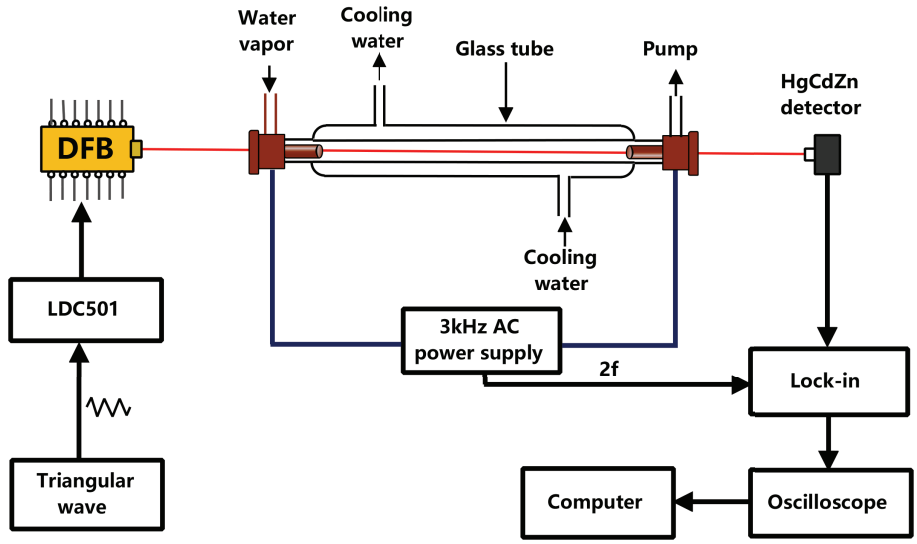

FIG. 1 Schematic diagram of concentration modulation spectroscopy. DFB: distributed feedback diode laser.

observed during the discharge. In this experiment, the CMS was used to suppress the absorption spectrum of stable molecules, thus enhancing the detection sensitivity for OH radicals and excited H_2O molecules. On the other hand, it was used to study the excitation and dissociation process of water molecules. The directions and demodulation phases of the observed spectral peaks were studied. This study attempts to understand the excitation and decomposition process of water vapor molecules.

II. THEORY OF CONCENTRATION MODULATION SPECTROSCOPY

In concentration modulation spectroscopy, the current of AC glow discharge is $i{=}i_m \sin(\omega t)$. If the lifetime of the transient molecule is very short, the concentration at a particular transition level completely follows the change of the discharge current. Therefore it can be expressed as

$$N(t) = N_0 + \Delta N_0 |\sin(\omega t)| \approx \Delta N_0 |\sin(\omega t)| \qquad (1)$$

Here N_0 is the number of background particles in a specific energy state, and ΔN_0 is the maximum amplitude of concentration change. $N_0{\approx}0$ can be a good approximation for the excited states of molecules, including the vibrational excited states. It can be seen from the above formula that for a sinusoidal modulated glow discharge with a period of $f{=}2\pi/\omega$, the particle number density changes periodically with a period of $2f$. Therefore, when $2f$ demodulation is used, the concentration modulation spectrum of the modulated transient molecules can be detected.

According to Beer-Lambert's law of absorption, the transmitted light intensity through the absorption cell is as follows:

$$I = I_0 \mathrm{e}^{-\sigma N(t) L} \qquad (2)$$

where L is the absorption path, σ is the absorption cross section of incident light for a specific transition, expressed as

$$\sigma = \frac{\lambda^2 \alpha(\nu - \nu_0)}{8\pi\tau} \qquad (3)$$

Here τ is the lifetime of the absorption state, $\alpha(\nu{-}\nu_0)$ is the absorption line shape, and ν_0 is the central frequency of the transition line. In the case of weak absorption, the transmitted light intensity is approximately described by $I{=}I_0(1{-}\sigma\Delta N_0|\sin(\omega t)|)L$. The optical signal is received by a photo detector and processed by the phase sensitivity lock-in amplifier at $2f$, and the output signal is as the following (assuming the time constant is T),

$$S(\nu) \approx I_0 \sigma \Delta N_0 l \lim_{T\to\infty} \frac{1}{2T} \times \int_{-T}^{T} |\sin(\omega t)| \sin(2\omega t + \theta) \mathrm{d}t \qquad (4)$$

where θ can be regarded as the phase angle of the lock-in amplifier. Herein, the signal is obtained at the optimum phase angle θ (ignoring higher-order terms greater than 2ω).

$$S(\nu) \propto I_0 \sigma \Delta N_0 l \propto I_0 \Delta N_0 l \alpha(\nu - \nu_0) \qquad (5)$$

Eq.(5) indicates that the measured signal of the concentration modulation spectrum is proportional to the maximum variation of the generated concentration ΔN_0.

DOI:10.1063/1674-0068/cjcp2001010

III. EXPERIMENTS

The experimental setup is shown in FIG.1. The concentration modulation spectra were probed by a MIR continuous-wave (2.8 μm) distributed feedback (DFB) diode laser (Nanoplus GmbH). A 0.7 Hz periodic triangular wave (generated by RIGOL DG811) was applied to tune the laser injection current, thus the laser wavenumber was scanned across the transitions of molecules. The temperature and current were controlled by a laser diode controller (Stanford Research LDC 501). After passing through an absorption cell, the laser was focused onto a photovoltaic detector (Vigo PVI-4TE-3.4). The absorption cell is a cylindrical discharge tube with a length of L=70 cm and an inner diameter of 1 cm. Water vapor was produced by injecting distilled water from a sealed container into the discharge cell at a pressure below the saturated pressure. The water vapor was discharged (Home-made AC supply) by copper electrodes at both ends of the tube to generate the concentration modulation of OH radical, and the discharge tube was cooled by distilled water outside to ensure uniform distribution of OH radicals. The discharge frequency was 3 kHz and the synchronous TTL signal was introduced to the lock-in amplifier (Stanford Resarch SR830) at the double discharge frequency ($2f$) for demodulation of OH radical. Signals from the lock-in were acquired with a digital oscilloscope (Tektronix MSO 2024B). The known wavenumber of OH and H_2O in HITRAN database [21] was used to calibrate the frequency of the observed spectrum.

IV. RESULTS AND DISCUSSION

A. Concentration modulation spectrum of OH

FIG. 2 shows the CMS measured by discharging the flowing water vapor. Six peaks were observed in CMS and their assignments are listed in Table I. Many other species were also generated during the discharge, but their absorption spectra were not observed because the laser was only about 2 cm^{-1}. The inset panel shows the normalized spectra of OH, the raw spectrum was normalized to the laser power so as to obtain the reliable spectral intensity. The atmospheric water vapor absorption background was eliminated and the CMS had a better resolution. The observed peaks are of Gaussian shape, but the background absorption of atmospheric water vapor at 3568.79816 cm^{-1} causes the spectral shape of this line in the cell to be different from that of other lines. Since the OH radicals have lower concentration compared to water vapor, the direct absorption spectroscopy can not detect the spectrum of OH. However, the CMS can pick up the spectrum of OH and achieve an enhanced detection sensitivity. Wavelength modulation absorption spectroscopy [19] and frequency modulation absorption spectroscopy [20] can both obtain enhanced sensitivity compared to direct absorption, but they cannot eliminate the background absorption of atmospheric water vapor. However, the combination of CMS and WMS may achieve both high sensitivity and selectivity to OH radicals.

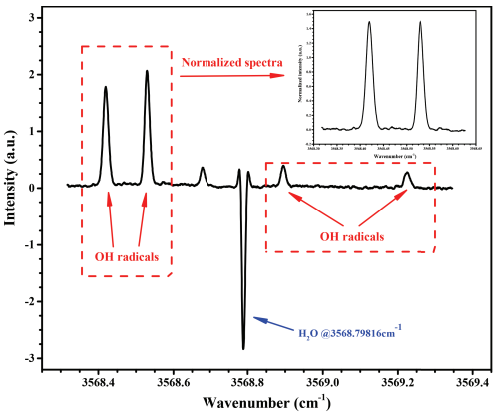

FIG. 2 A portion of concentration modulation absorption spectrum of OH and H_2O absorption, the inset shows the normalized spectrum of OH radicals.

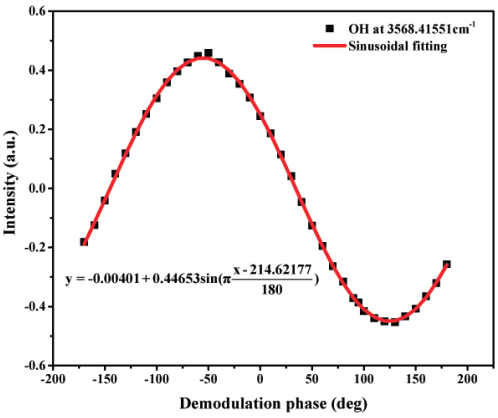

FIG. 3 Relationship between OH relative intensity and demodulation phase at 3568.41551 cm^{-1}.

B. Population change discrimination using demodulation phase

The observed peaks in FIG.2 have opposite directions: one peak of water vapor directs downward, and the others are upward. When demodulation is performed using a lock-in amplifier, the intensity and orientation of the peak is proportional to $\sin(\Delta\phi)$, where $\Delta\phi$ is the phase difference between the reference phase and the phase of the input signal. As a result, the observed intensity will vary with the reference phase in sine function. FIG. 3 shows the spectral intensity of OH ($Q_{ef}(1.5)$) at different reference phase. The observed intensity was fitted to sine function and a good agreement

DOI:10.1063/1674-0068/cjcp2001010

TABLE I The line list of OH and H_2O studied in this work [21].

Molecule	Line/cm^{-1}	Assignment	Description	Phase shift/cm^{-1}
OH	3568.41551	$X_{3/2}$(1 1.5 F_1 e)←$X_{3/2}$(0 1.5 F_1 f)	Q_{ef}(1.5)	214.6
OH	3568.52242	$X_{3/2}$(1 1.5 F_1 f)←$X_{3/2}$(0 1.5 F_1 e)	Q_{fe}(1.5)	220.2
H_2O	3568.67889	011 5 3 2←010 6 3 3		231.4
H_2O	3568.79816	100 4 2 3←000 4 3 2		34.1
OH	3568.90555	$X_{1/2}$(1 0.5 F_2 e)←$X_{1/2}$(0 0.5 F_2 f)	Q_{ef}(0.5)	216.0
OH	3569.21414	$X_{1/2}$(1 0.5 F_2 f)←$X_{1/2}$(0 0.5 F_2 e)	Q_{fe}(0.5)	216.8

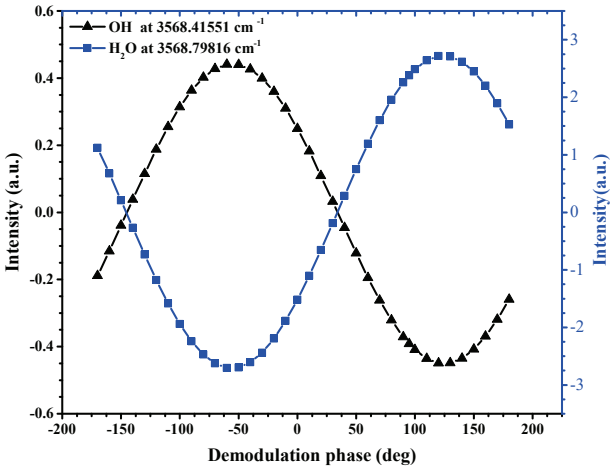

FIG. 4 Relationship between relative spectral intensities and demodulation phase for OH and H_2O.

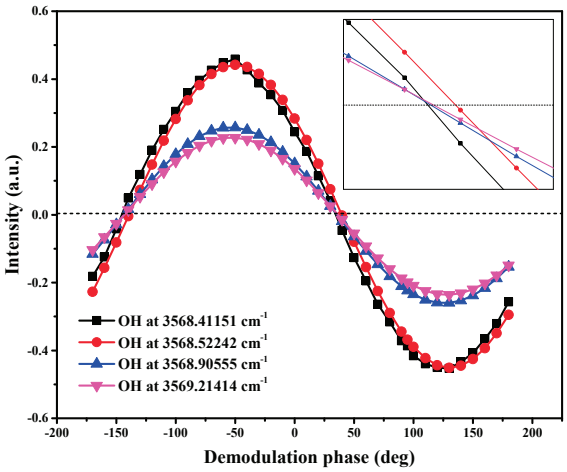

FIG. 5 Spectral intensities of four OH peaks dependence on the demodulated phase.

was obtained. The fitting function is as follows

$$y = y_0 + A \times \sin\left[\pi\left(\frac{x - x_c}{w}\right)\right] \tag{6}$$

where w is the period and its value was fixed at 180°; x_c is the phase shift and the fitted values of x_c of the six peaks are listed in Table I.

The spectral intensities were measured at different reference phases to find the reasons for the different orientations of these peaks. FIG. 2 maximizes the spectral intensity of OH by optimizing the reference phase of the lock-in amplifier. It is found that the intensity of one peak of water vapor is also near its maximum value, but the direction of its absorption peak is opposite to that of other absorption peaks.

FIG. 4 shows the spectral intensities associated with the reference phases of OH (Q_{ef}(1.5)) and H_2O (υ_1: 4_{23}←4_{32}). At fist glance, the phase shift (x_c) of H_2O is about 180° different from that of OH radical. The fitting phase are 214.6° and 34.1° for OH and H_2O, respectively. The phase difference is 180.5°, which results in the opposite direction of the peaks. The reason for this opposition or phase difference is that OH is generated by discharging water. The concentration of OH is kept in synchronization with the external modulation field. At the same time, the peak of H_2O comes from the ground (0 0 0) state. In the discharge process, stable water vapor molecules are continuously pumped to the higher energy levels, some of which are dissociated into OH molecules. This means that the increase of OH is accompanied by the decrease of ground state water vapor molecules.

The water vapor molecules on its ground state will also be pumped to the excited state during the discharge process. Therefore, the water vapor absorption peaks of some excited states will increase, and the phase difference of peaks between excited states and ground state is nearly 180°. As for this study, the phase shift difference of the two peaks of water vapor is 197.3° (231.4° and 34.1°), as shown in Table I. The phase difference is not close to 180°, indicating that the concentration change of excited state lags behind the ground state in the discharge process.

The detailed study shows that the phase shifts of the four OH peaks are also different. This difference is shown in FIG. 5, and the specific values are shown in Table I. By sine fitting, the phase difference of OH Q(1.5) double lines is 5.6°. In the concentration modulation spectroscopy, the lifetime of the transition is usually the reason that affects the different demodulation phase. But in this study, the lifetimes of OH Q(1.5) double lines are almost the same [21]. Therefore, the

DOI:10.1063/1674-0068/cjcp2001010

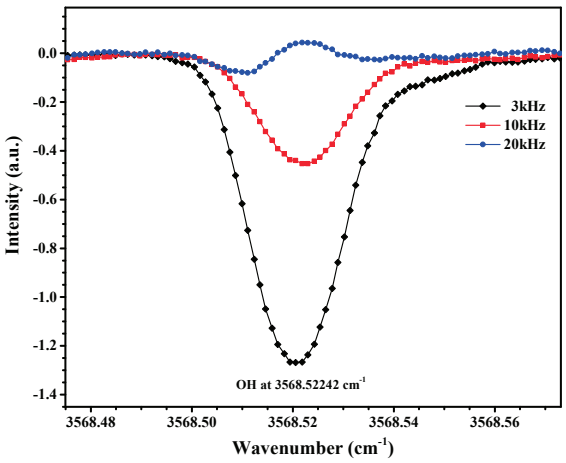

FIG. 6 Spectra of OH at 3568.52242 cm^{-1} observed at different discharge frequency.

difference of lifetimes is only one possible reason for the difference of demodulation phases.

Another reason for this phase difference may be that the generation and release of population in the lower energy levels are different. In the process of discharge, the population of the lower levels may come from different channels. In addition, the population of the lower levels may also be released through different channels. The different channels of generation and release may lead to the difference of the concentration modulation process, and also lead to the incomplete synchronization of external electric field.

In this study, OH is produced by the discharge of water vapor molecules. The population of all levels of OH is positively related to the absolute value of voltage, so the directions of absorption peak are the same. However, the population channels or release channels of different levels of OH molecules are different, and the demodulation phases may be slightly different. The voltage in-homogeneity during the discharge process may be another reason for this slight phase difference.

C. Lifetime estimation using concentration modulation

The spectral intensity of OH molecules is related to the modulation frequency of concentration modulation. FIG. 6 shows the OH concentration modulation spectrum observed under the same conditions, except for the different frequencies of 3, 10, and 20 kHz. The spectrum intensity obtained at 3 kHz is stronger than the other two, and the spectrum with ideal line shape cannot be obtained at 20 kHz.

The CMS is highly sensitive to short-lived molecules, since the concentration or population modulation regulates the formation of transient molecules, long lived or stable molecules will not be modulated and will not be detected. As for OH radical, the energy levels at its ground state have relatively long lifetime. When the modulation frequency is too high, the period of excitation and relaxation is very small. If the modulation period is less than the lifetime of the levels, the populations on the energy level will not be fully modulated. This means that in the second excitation, the previous population is not released completely, but with a stable population.

By tuning the modulation frequency and monitoring the spectral intensity, it is possible to roughly estimate the energy level lifetime of the transient species. As shown in FIG. 6, when the modulation frequency increases from 3 kHz, 10 kHz to 20 kHz, the spectral intensity increases continuously. This means that the lifetime of OH ($X_{3/2}(\upsilon=0)$) state is more than 50 μs (the concentration of OH is modulated at 20 kHz). Although the maximum spectral intensity was observed at 3 kHz, we can not determine the accurate lifetime of OH limited by the modulation frequencies. The relatively accurate lifetime may be determined by a frequency adjustable discharge system. In a specific experimental environment, the optimal modulation frequency should be close to the lifetime of the electronic states of molecules.

V. CONCLUSION

The population change of the energy levels of OH and H_2O was determined through the orientations of the measured spectral peaks using CMS. Using the orientation of the peaks, we can judge whether the population of H_2O increases or decreases at a specific energy level. The increase or decrease of the population in the molecular energy levels will result in a 180° difference in the optimal demodulation phases. Since OH is one of the products of H_2O discharge, its optimal demodulation phase is of 180° difference from the lower state of H_2O. The slightly phase difference of the spectrum of OH may come from the different excitation and relaxation progresses. The dynamic process of excitation, ionization and decomposition of water vapor molecules may be studied if a broad spectral region can be observed and more transient species can be monitored.

VI. ACKNOWLEDGMENTS

This work was supported by the National Natural Science Foundation of China (No.61625501, No.61427816), the Open Fund of the State Key Laboratory of High Field Laser Physics (SIOM), and the Open Fund of the State Key Laboratory of Precision Spectroscopy.

[1] B. Sun, M. Sato, and J. S. Clements, J. Electrost. **39**, 189 (1997).

[2] R. G. Prinn, J. Huang, R. F. Weiss, D. M. Cunnold, P. J. Fraser, P. G. Simmonds, A. McCulloch, C. Harth, P. Salameh, S. O'Doherty, R. H. J. Wang, L. Porter, and B. R. Miller, Science **292**, 1882 (2001).
[3] Y. Kanaya, Y. Sadanaga, J. Hrokawa, Y. Kajii, and H. Akimoto, J. Atmos Chem. **38**, 73 (2001).
[4] Q. Xiong, Z. Q. Yang, and P. J. Bruggeman, J. Phys. D **48**, 424008 (2015).
[5] S. L. Yao, S. Weng, Y. Tang, C. W. Zhao, Z. L. Wu, X. M. Zhang, S. Yamamoto, and S. Kodama, Vacuum **126**, 16 (2016).
[6] A. N. Heays, N. de Oliveira, B. Gans, K. Ito, S. Boye-Peronnec, S. Douin, K. M. Hickson, L. Nahon, and J. C. Loison, J. Quant Spectrosc. Radiat. Transf. **204**, 12 (2018).
[7] S. K. Wang and R. K. Hanson, Opt. Lett. **43**, 3518 (2018).
[8] A. Sarani, A. Y. Nikiforov, and C. Leys, Phys. Plasmas **17**, 063504 (2010).
[9] R. Ono and T. Oda, J. Phys. D **35**, 2133 (2002).
[10] C. H. Zhou, S. B. Cheng, H. M. Yin, and G. Z. He, Chin. J. Chem. Phys. **22**, 681 (2009).
[11] S. Kanazawa, H. Kawano, S. Watanabe, T. Furuki, S. Akamine, R. Ichiki, T. Ohkubo, M. Kocik, and J. Mizeraczyk, Plasma Sources Sci. Technol. **20**, 034010 (2011).
[12] S. R. Plimpton, M. Gokowski, D. G. Mitchell, C. Austin, S. S. Eaton, G. R. Eaton, C. Gokowski, M Voskuil, Biotechnol. Bioeng. **110**, 1936 (2013).
[13] Y. Gorbanev, D. O'Connell, and V. Chechik, Chem. Eur. J. **22**, 3496 (2016).
[14] C. Miron, M. A. Bratescu, N. Saito, and O. Takai, J. Appl. Phys. **109**, 123301 (2011).
[15] P. Bruggeman, G. Cunge, and N. Sadeghi, Plasma Sources Sci. Technol. **21**, 035019 (2012).
[16] G. Dilecce, P. F. Ambrico, M. Simek, and S. De Benedictis, J. Phys. D **45**, 125203 (2012).
[17] C. S. Gudeman, M. H. Megemann, J. Pfaff, and R. J. Saykally, Phys. Rev. Lett. **50**, 727 (1983).
[18] S. K. Stephenson and R. J. Saykally, Chem. Rev. **105**, 3220 (2005).
[19] X. Q. Guo, F. Zheng, C. L. Li, X. F. Yang, N. Li, S. P. Liu, J. L. Wei, X. B. Qiu, and Q. S. He, Opt. Laser Eng. **115**, 243 (2019).
[20] C. L. Li, L. G. Shao, H. Y. Meng, J. L. Wei, X. B. Qiu, Q. S. He, W. G. Ma, L. H. Deng, and Y. Q. Chen. Opt. Express **26**, 29330 (2018).
[21] I. E. Gordon, L. S. Rothman, C. Hill, R. V. Kochanov, Y. Tan, P. F. Bernath, M. Birk, V. Boudon, A. Campargue, K. V. Chance, B. J. Drouin, J. M. Flaud, R. R. Gamache, J. T. Hodges, D. Jacquemart, V. I. Perevalov, A. Perrin, K. P. Shine, M. A. H. Smith, J. Tennyson, G. C. Toon, H. Tran, V. G. Tyuterev, A. Barbe, A. G. Csaszar, V. M. Devi, T. Furtenbacher, J. J. Harrison, J. M. Hartmann, A. Jolly, T. J. Johnson, T. Karman, I. Kleiner, A. A. Kyuberis, J. Loos, O. M. Lyulin, S. T. Massie, S. N. Mikhailenko, N. Moazzen-Ahmadi, H. S. P. Mueller, O. V. Naumenko, A. V. Nikitin, O. L. Polyansky, M. Rey, M. Rotger, S. W. Sharpe, K. Sung, E. Starikova, S. A. Tashkun, J. Vander Auwera, G. Wagner, J. Wilzewski, P. Wcislo, S. Yu, and E. J. Zak, J. Quant Spectrosc. Radiat. Transf. **203**, 3 (2017).

DOI:10.1063/1674-0068/cjcp2001010